



Original Article

Salicylic acid fights against *Fusarium* wilt by inhibiting target of rapamycin signaling pathway in *Fusarium oxysporum*

Linxuan Li ^{a,b,c,1}, Tingting Zhu ^{a,b,c,1}, Yun Song ^{d,1}, Li Feng ^{a,b,c}, Philip James Kear ^e, Rooallah Saberi Riseh ^f, Mahmoud Sitohy ^g, Raju Datla ^h, Maozhi Ren ^{a,b,c,*}

^aInstitute of Urban Agriculture, Chinese Academy of Agricultural Sciences, Chengdu National Agricultural Science and Technology Center, Chengdu 610000, China

^bZhengzhou Research Base, State Key Laboratory of Cotton Biology, School of Agricultural Science of Zhengzhou University, Zhengzhou 450000, China

^cHainan Yazhou Bay Seed Laboratory, Sanya 572025, China

^dSchool of Life Sciences, Liaocheng University, Liaocheng 252000, China

^eInternational Potato Center (CIP) China Center Asia Pacific, Beijing 100000, China

^fDepartment of Plant Protection, Faculty of Agriculture, Vali-e-Asr University of Rafsanjan, Rafsanjan, Iran

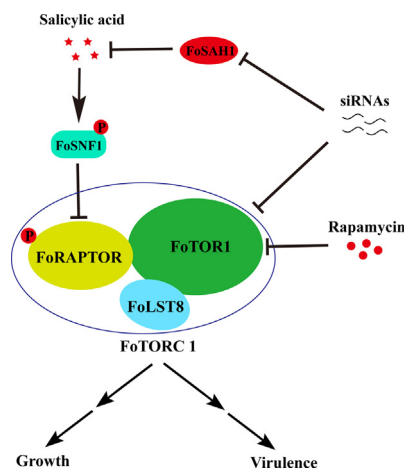
^gBiochemistry Department, Faculty of Agriculture, Zagazig University, Zagazig 44511, Egypt

^hGlobal Institute for Food Security in Saskatoon, University of Saskatchewan, Saskatoon S7N0W9, Canada

HIGHLIGHTS

- Isolating and sequencing the genome of *F. oxysporum* from potato tubers with dry rot symptoms.
- SA efficiently arrests hyphal growth, sporular production and pathogenicity of *F. oxysporum*.
- SA inhibits the activity of FoTORC1 via activating FoSNF1 in *F. oxysporum*.
- Transgenic potato plants with interference of *FoTOR1* and *FoSAH1* genes prevent the occurrence of *Fusarium* wilt.
- Providing insights SA into controlling various fungal diseases by targeting the SNF1-TORC1 pathway of pathogens.

GRAPHICAL ABSTRACT



ARTICLE INFO

Article history:

Received 6 July 2021

Revised 11 October 2021

Accepted 28 October 2021

Available online 02 November 2021

Keywords:

Salicylic acid

Target of rapamycin

Hyphal growth

ABSTRACT

Introduction: Biofungicides with low toxicity and high efficiency are a global priority for sustainable agricultural development. Phytohormone salicylic acid (SA) is an ancient medicine against various diseases in humans and activates the immune system in plants, but little is known of its function as a biofungicide. **Objectives:** Here, *Fusarium oxysporum*, the causal agent of devastating *Fusarium* wilt and immunodepressed patients, was used as a model system to explore whether SA can enter the pathogen cells and suppress key targets of the pathogen.

Methods: Oxford Nanopore MinION sequencing and high-throughput chromosome conformation capture (Hi-C) sequencing were used to analyze the genome of *F. oxysporum*. In addition, RNA-seq, qRT-PCR, and western blotting were conducted to detect gene and protein expression levels.

Peer review under responsibility of Cairo University.

* Corresponding author at: Institute of Urban Agriculture, Chinese Academy of Agricultural Sciences, Chengdu National Agricultural Science and Technology Center, Chengdu 610000, China.

E-mail address: renmaozhi01@caas.cn (M. Ren).

¹ These authors contributed equally.

<https://doi.org/10.1016/j.jare.2021.10.014>

2090-1232/© 2022 The Authors. Published by Elsevier B.V. on behalf of Cairo University.

This is an open access article under the CC BY-NC-ND license (<http://creativecommons.org/licenses/by-nc-nd/4.0/>).

Pathogenicity
Fusarium oxysporum

Results: We isolated and sequenced the genome of *F. oxysporum* from potato dry rot, and the *F. oxysporum* included 12 chromosomes and 52.3 Mb genomic length. Pharmacological assays showed that exogenous application of SA can efficiently arrest hyphal growth, spore production, and pathogenicity of *F. oxysporum*, whereas endogenous salicylate hydroxylases significantly detoxify SA. The synergistic growth inhibition of *F. oxysporum* was observed when SA was combined with rapamycin. Kinase assays showed that SA inhibits FoTOR complex 1 (FoTORC1) by activating FoSNF1 in vivo. Transgenic potato plants with the interference of *FoTOR1* and *FoSAH1* genes inhibited the invasive growth of hyphae and significantly prevented the occurrence of *Fusarium* wilt.

Conclusion: This study revealed the underlying mechanisms of SA against *F. oxysporum* and provided insights into SA in controlling various fungal diseases by targeting the SNF1-TORC1 pathway of pathogens.

© 2022 The Authors. Published by Elsevier B.V. on behalf of Cairo University. This is an open access article under the CC BY-NC-ND license (<http://creativecommons.org/licenses/by-nc-nd/4.0/>).

Introduction

The use of chemical fungicides has substantially increased in the past few decades. Chemical fungicides are necessary to control fungal diseases in agricultural crops. However, health risks, food safety hazards, and water and soil pollution resulting from chemical fungicide residues are a global challenge [1,2]. Infants and children are particularly vulnerable to chemical fungicide residues. The bioaccumulation of chemical residues can be magnified through the food chain and quickly reaches a harmful level in the human body. Biofungicides with low toxicity and high efficiency are required for food safety, human health and sustainable development.

Phytohormone salicylic acid (SA) is an ancient medicine made from willow bark. It has been used against fever, pain, and inflammation since ancient Egypt [3]. SA can activate adenosine monophosphate-activated protein kinase (AMPK), an important regulator of cell growth and metabolism [4,5]. Activated AMPK directly phosphorylates RAPTOR at the conserved serine residue (Ser792) and inhibits TORC1 activity in animals and humans [6]. In plants, SA plays a vital role in activating plant disease resistance systems, including pattern-triggered immunity, effector-triggered immunity, and systemic acquired resistance [7,8]. In addition, previous studies have shown that SA enhances antifungal activity by inhibiting hyphal growth and spore germination in *Fusarium oxysporum*, *Magnaporthe grisea*, and *Penicillium expansum* [9–12]. However, molecular mechanism of SA function as a biofungicide targeting plant pathogens is unclear.

Fusarium wilt, caused by *Fusarium oxysporum*, is one of the most devastating plant diseases worldwide [13,14]. Due to the soil-borne and vascular plant colonization feature of *F. oxysporum*, a high dosage of chemical fungicides with high toxicity is required to control *Fusarium* wilt. More than 100 plants, for example, banana, potato, cotton, and tomato, are severely affected by this pathogen [15–17], globally resulting in tremendous economic losses. However, limited progress has been made in finding effective biofungicides for controlling *Fusarium* wilt disease.

Target of rapamycin (TOR) is an evolutionarily conserved Ser/Thr protein kinase in eukaryotes. The TOR signaling pathway regulates cell growth, metabolism, and proliferation in response to nutrients, energy, and stresses [18–20]. Rapamycin (RAP) is a macrolide immunosuppressant produced by *Streptomyces hygroscopicus*. It can mimic nutrient limitations to arrest cell growth and proliferation. RAP specifically interacts with FKBP12 to prevent TOR from associating with its scaffold protein RAPTOR (regulatory associate protein of TOR) [21,22], which hinders TOR protein activity and results in irreversibly arresting the G1 phase of the cell cycle [23].

Potato is a primary staple food worldwide, but potato *Fusarium* wilt and dry rot diseases caused by *F. oxysporum* are global

challenges for potato production. In this study, the potato / *F. oxysporum* system was employed as a model system to reveal new functions of SA against vascular fungal diseases. We isolated and identified the pathogenic fungus *F. oxysporum* from potato tubers with dry rot symptoms, and further inoculation assays showed that the pathogen could infect a wider range of crops. Genome sequencing and chromosome assembly showed that the *F. oxysporum* contained 12 chromosomes and 52.3 Mb genomic length. We found that the phytohormone SA inhibited FoTORC1 signaling by activating FoSNF1 (FoAMPK α) and then phosphorylating FoRAPTOR, resulting in arrested mycelial growth, spore production, and virulence of *F. oxysporum*. However, endogenous salicylate hydroxylase (FoSAH1) significantly attenuated the toxicity of exogenous SA. Additionally, the synergistic growth inhibition of *F. oxysporum* was generated when SA was combined with RAP. Transgenic plants with *FoTOR1* and *FoSAH1* RNA interference significantly prevented the occurrence of *Fusarium* wilt. Our results demonstrated that SA could function as a novel biofungicide to control fungal diseases such as *Fusarium* wilt by targeting the FoSNF1-FoTORC1 signaling pathway.

Material and methods

Fungal strains and culture conditions

The wild-type (WT) strain (*Fo-4*) was isolated from Chongqing local potato with dry rot symptoms. *Fusarium oxysporum* f. sp. *lycopersici* (*Fol*) strain comes from BeNa Culture Collection (BNCC, Beijing, China; BNCC114534) in this study. The *Fo-4* strain, deletion mutant strains, and complementary strains were routinely cultured on potato dextrose agar (PDA) at 27 °C. To extract genomic DNA and RNA of *F. oxysporum*, hyphae were incubated in potato dextrose broth (PDB) for four days at 27 °C with shaking (Incubator shaker, MQT-60R, China) at 160 rpm.

Genome sequencing and assembly

DNA of *Fo-4* strain was isolated by CTAB method. Libraries were built using the Ligation Sequencing Kit 1D (SQK-LSK108) from Oxford Nanopore. MinION sequencing was performed following the manufacturer's standard protocol and sequenced to achieve approximately 170X sequencing coverage. wtdbg2 software was used to assemble the reads after error correction [24]. The genomic assembly completeness of polished contigs was evaluated by BUSCO v2.0 [25].

Hi-C sequencing

According to the Hi-C procedure, nuclear DNA from the mycelium of *Fo-4* was cross-linked and then cut with a restriction

enzyme. Illumina sequencing (150 bp paired-end) was performed on a HiSeq with ~100X coverage. After reads filtering, we obtained 12.57 million valid interaction pairs for the chromosome-level assembly of *Fo-4*. The contigs within the assemblies were separately broken into fragments with a length of 50 Kb and were then clustered by LACHESIS software [26]. Thirty-three contigs with total lengths of 51.7 Mb were anchored and oriented to 12 chromosome-level groups. The mitochondrial DNA was assembled from Illumina sequencing reads using GRAB software [27].

Construction of vectors for gene deletion and complementation

The primers used to amplify the flanking sequences or CDS of each gene were listed in Table S9. Constructs for gene deletion and complementation of *Fo-4* were carried out as described previously [28]. Transgenic *F. oxysporum* was produced by *Agrobacterium*-mediated genetic transformation. The *Agrobacterium tumefaciens* strain AGL-1 containing deletion or complementation vectors was grown at 28 °C in LB liquid medium until the OD₆₀₀ reached 0.8. The culture was diluted to OD₆₀₀ = 0.25 in the induction medium contains 200 μM acetosyringone and cultured for 6 h at 28 °C, 180 rpm on a shaker (Incubator shaker, MQT-60R, China). Mixing with an equal volume of the conidial suspension of *F. oxysporum* (10⁷ conidia mL⁻¹). Then, 300 μL of the mixture was placed onto nitrocellulose filters (pore size, 0.45 μm; diameter, 80 mm) on co-cultivation medium for 48 h. The filters subsequently were transferred to selective medium containing antibiotic and cefotaxime. After seven days, selected transformants were transferred to fresh PDA medium with antibiotic.

Yeast two-hybrid assay

To construct plasmids for yeast two-hybrid analyses, the coding sequences of genes were amplified from the cDNA of *Fo-4*. The genes were inserted into pGBKT7 and pGADT7 vectors (Clontech, CA, USA). The pairs of yeast two-hybrid plasmids were co-transformed into *Saccharomyces cerevisiae* strain Y2HGold following the PEG/LiAc transformation protocol (Clontech, Cat. No. 630489). Transformants were grown at 28 °C for five days on a synthetic medium lacking Leu and Trp, and then colonies were transferred to synthetic medium lacking His, Leu, Ade and Trp supplemented with 40 μg/mL X-a-Gal and 200 ng/mL Aureobasidin A.

Western blotting analysis

For western blotting of *Fo-4*, hyphae were treated with different concentrations of SA and total protein extracts were prepared with RIPA lysis buffer. Primary antibodies were used: rabbit anti-phospho-AMPKα T172 (#2535; Cell signaling technology), mouse anti-AMPKα (MCA2672GA; BIO-RAD), rabbit anti-phospho-RAPTOR S792 (#2083; Cell signaling technology), rabbit anti-RAPTOR (#2280; Cell signaling technology), rabbit anti-phospho-S6 ribosomal protein S235/236 (#2211; Cell signaling technology), rabbit anti-RPS6 (ab40820; Abcam), and mouse anti-yeast β-actin (AT0014; CMCTAG). The integrated optical density values of the indicated bands were quantified using the software Image-Pro Plus.

Expression profiling sequencing and analysis

Hyphae of *Fo-4* were grown for four days in PDB medium at 27 °C with shaking at 160 rpm, and then treated with 5 mM SA and DMSO (as a control) for 12 h, respectively. Total RNA of *Fo-4* mycelium was isolated using the RNAprep Pure Fungi Kit (TIANGEN, Beijing, China). For each treatment, three independent biolog-

ical replicates were performed. An Illumina HiSeq 2000 platform was used to sequence the cDNA library. The clean reads were mapped to the reference *F. oxysporum* genome by using TopHat2 software. Cuffdiff was used to identify differentially expressed genes (DEGs). Gene ontology (GO) enrichment (corrected P value < 0.05) of the differentially expressed genes was performed by using Goseq software. The enrichment of DEGs in Kyoto Encyclopedia of Genes and Genomes pathways (corrected P value < 0.05) was obtained by KOBAS software [29].

Quantitative real-time PCR

Total RNA of *Fo-4* mycelium was isolated using the RNAprep Pure Fungi Kit (TIANGEN, Beijing, China). cDNA was synthesized from total RNA using the TransScript[®] Reverse Transcriptase (TransGen, Beijing, China). Relative transcript levels were tested by the CFX96 real-time PCR system (BIO-RAD, USA). Relative transcript level of target gene was calculated by 2^{-ΔΔCt}. Real-time primers were presented in Table S9. The *F. oxysporum* translation elongation factor 1 alpha (*FoEF1α*) and *Actin1* (*FoACT1*) genes were used as internal control. The data represents the mean ± SD of three independent experiments.

Combination index (CI) value measurement

Combination index (CI) values were used to quantitatively measure the interaction between SA and RAP. The degree of reagent interaction is based on synergism (CI < 1), additive effect (CI = 1), or antagonism (CI greater than 1) [30]. Hyphae of *Fo-4* were incubated on PDA medium including different concentrations of SA, RAP, and combinations of SA and RAP for six days at 27 °C. Colony diameter was measured to calculate growth inhibition. Experiments were repeated three times. Affected fraction (Fa) represented the percentage of colony diameter affected by drug and was calculated by (1-T/C) × 100%. C: colony diameter of control, T: colony diameter of drug-treatment.

Pathogen inoculation assay

Pathogen inoculation was performed by point-inoculated on the surface of potato leaves and tubers with conidia of *Fo-4* (10⁷ conidia mL⁻¹) as described previously [31]. Inoculated leaves and tubers were cultured on moist filter paper at 27 °C in a long daylight condition for four days. At least ten leaves and tubers of each line were treated every time. The experiment was repeated three times.

Statistical analyses

Two-tailed Student's t-tests and two-way ANOVA were performed using the IBM SPSS statistics software to investigate the statistical differences between control and other samples. Different letters represented significant differences between treatments (Tukey, p < 0.05) in the two-way ANOVA. Significant differences between control and other samples were indicated by one (*P < 0.05) or two (**P < 0.01) asterisks in the two-tailed Student's t-tests.

Data availability

The RNA-seq and genome data have been deposited in the NCBI Sequence Read Archive under accession numbers PRJNA730676 and PRJNA730382, respectively. The ITS sequences of *Fo-2* and *Fo-4* have been deposited in the NCBI GenBank accession numbers MZ208819 and MZ223468, respectively. Other relevant data are available in supplemental materials.

Results

Genome sequencing and assembly of *F. oxysporum*

Fusarium oxysporum, one of the most destructive fungal pathogens resulting in *Fusarium* wilt and dry rot in potato, was used as a model system to test whether SA can directly inhibit its growth. Two *F. oxysporum* (*Fo*) strains were isolated and identified from potato tubers with dry rot symptoms (Fig. S1a). Severe potato *Fusarium* dry rot infections were observed in *Fo*-2 and *Fo*-4 strains when inoculated on potato tubers, indicating that *Fo*-2 and *Fo*-4 strains are the causal agents of potato *Fusarium* dry rot (Fig. S1b). The DNA sequencing results of internal transcribed spacer (ITS) showed that *Fo*-2 and *Fo*-4 strains belong to the *F. oxysporum*, close to *Fusarium oxysporum* f. sp. *tuberosi* and *Fusarium oxysporum* f. sp. *lycopersici* (*Fol*) *forma specialis* (Fig. S1c). Because *Fo*-2 and *Fo*-4 strains showed highly consistent growth patterns and genetic features, the *Fo*-4 strain was selected for subsequent research. To test whether *F. oxysporum* can infect other crops, *Fo*-4 and *Fol* strains were point-inoculated onto the surface of several economically crops. Interestingly, *Fo*-4 rather than *Fol* was observed to infect many economically crops ranging from citrus, Chinese yam, tomato, grape, banana, pachyrhizus to cucumber (Fig. S2), indicating that *Fo*-4 does not show *forma specialis* as the most of pathological *F. oxysporum* species [16].

To advance the understanding of *Fo*-4 and other *F. oxysporum* species, we sequenced the whole genome of *Fo*-4 using the Nanopore sequencing platform. A total of ~8.9 Gb clean reads were obtained with a sequencing depth of 170x, and the total genome length was assembled to 52.3 Mb (Table S1). The genome encodes 17,406 genes, and the GC content of the genome is 47.28%. In contrast with the high content of repetitive sequences in the *Fol* (4287) genome, approximately 6.37% of the entire *Fo*-4 genome was identified as repeat sequences, including many *retro*-elements, short and long interspersed nuclear elements, and DNA transposons.

Chromosome level ordering of the scaffolds was achieved by high-throughput chromosome conformation capture (Hi-C). A Hi-C heatmap indicated that the assembled genome of *Fo*-4 had 12 chromosomes and a mitochondrial chromosome, and 51.7 Mb genomic sequences were mapped to these chromosomes (Fig. S3). Eleven conserved chromosomes were identified through synteny analysis of orthologous genes between *Fo*-4 and *Fol* (4287). However, chromosome 11 and contig00016 did not show clear synteny with the *Fol* (4287) chromosomes (Fig. 1). Furthermore, chromosome 11 and contig00016 contain many repetitive sequences, suggesting that chromosome 11 and contig00016 have greater variability in the *Fo*-4 strain.

Exogenous SA significantly inhibits the mycelial growth and pathogenicity of *F. oxysporum*

To examine the effects of SA on the growth of *F. oxysporum*, *Fo*-4 was treated with different concentrations of SA. Hymexazol fungicide, widely used for *Fusarium* wilt control, was used as a positive control. The growth inhibition of *F. oxysporum* positively correlated with SA dose, and the IC_{50} (half-maximal inhibitory concentration) value of SA was 5 mM (Fig. 2a and c). The hyphal growth of *F. oxysporum* was completely inhibited when the concentration of SA reached 10 mM, which was similar to hymexazol fungicide at 5 μ L mL⁻¹ (Fig. 2a). To examine whether the defective phenotype of hyphal growth can be restored by removing SA and hymexazol from the PDA medium, the SA- and hymexazol-treated *F. oxysporum* hyphae were transferred to PDA medium plates and grown for four days (Fig. S4). The results showed that 15 mM SA- and 10 μ L mL⁻¹ hymexazol-treated *F. oxysporum* hyphae could not be

rescued on the drug free PDA medium, indicating that SA can function as a biofungicide to cause cell death in *F. oxysporum*. Next, the ability of SA to damage the ultrastructure of *F. oxysporum* was investigated. The scanning electron microscope (SEM) results showed distorted and swollen hyphae and shorter hyphal septa of *F. oxysporum* caused by SA treatment (Fig. 2b). This result suggested that SA induced hyphal cell death in *F. oxysporum*, causing the deficient growth phenotypes. Notably, the spore production of *F. oxysporum* was also significantly decreased in a SA dose-dependent manner (Fig. 2d). These observations demonstrated that SA could mimic chemical fungicides to cause cell death of *F. oxysporum*.

To test the pathogenicity of *F. oxysporum* treated with SA in potato, spores were mixed with different concentrations of SA and then point-inoculated on the surface of potato leaves and tubers. As expected, SA inhibited *Fusarium* wilt lesions caused by *F. oxysporum* in a dose-dependent manner, reducing the fungal biomass, shrinking the necrosis symptoms, and slowing down yellowness and wilting (Fig. 2e-g). These results indicated that SA inhibited the hyphal growth and pathogenicity of *F. oxysporum*.

SA affects various biological processes in *F. oxysporum*

To further elucidate the function of SA on vegetative growth and cell metabolism of *F. oxysporum*, RNA-seq was performed in *F. oxysporum* with DMSO and SA treatment (Fig. 3a). A total of 5762 differentially expressed genes (DEGs) were found between DMSO control and SA treatment, of which 2801 DEGs were downregulated and 2961 DEGs were upregulated (Fig. 3b and c). Gene ontology (GO) enrichment analysis was performed to identify the biological functions of the DEGs found between SA and DMSO. A total of 368 upregulated GO terms and 285 downregulated GO terms were enriched in the RNA-seq data (Table S2). Among these GO terms, peptide metabolic process, cellular amide metabolic process, and peptide biosynthetic process were the most significant enrichment (Fig. 3d). Pathway enrichment analysis showed that SA affects multiple metabolic pathways, including carbon metabolism, ribosome, and biosynthesis of secondary metabolites (Fig. 3e). The most significant enrichment pathway was the biosynthesis of secondary metabolites. There were 230 DEGs in the biosynthesis of secondary metabolites, most of which were significantly upregulated (Table S3). Furthermore, these DEGs mainly regulated the biosynthesis of type II polyketide backbone and products, polyketides and nonribosomal peptides, and nonribosomal peptide structures in the biosynthesis of secondary metabolites (Fig. S5).

Next, we analyzed the effect of SA on the pathogenicity-related genes of *F. oxysporum*. Through analysis of gene expression profile data, we found 24 DEGs associated with mitogen-activated protein kinase (MAPK) signaling pathway, including 19 downregulated genes and 5 upregulated genes (Fig. S6 and Table S4). Previous studies showed that MAPK signaling pathway had important functions in hyphal infection, appressorium formation, cell wall integrity, stress response, and virulence of phytopathogenic fungi [32]. The MAPKs *Fmk1* and *Hog1* have been shown to control invasive growth and pathogenicity in *F. oxysporum* [33,34]. Transcriptome data showed that the transcription levels of *Fmk1* (*FOXG_08140*) and *Hog1* (*FOXG_06318*) were downregulated 0.57- and 0.48-fold in SA-treated hyphae, respectively (Table S4). In addition, cell wall degrading enzymes (CWDEs) produced by phytopathogenic fungi were proved to be virulence factors involved in fungal infection processes [35,36]. CWDEs, including cellulases, xylanases and pectinases, were changed under SA treatment in the RNA-seq data (Table S5). Notably, most of the differentially expressed CWDE genes were significantly downregulated. The transcriptome results

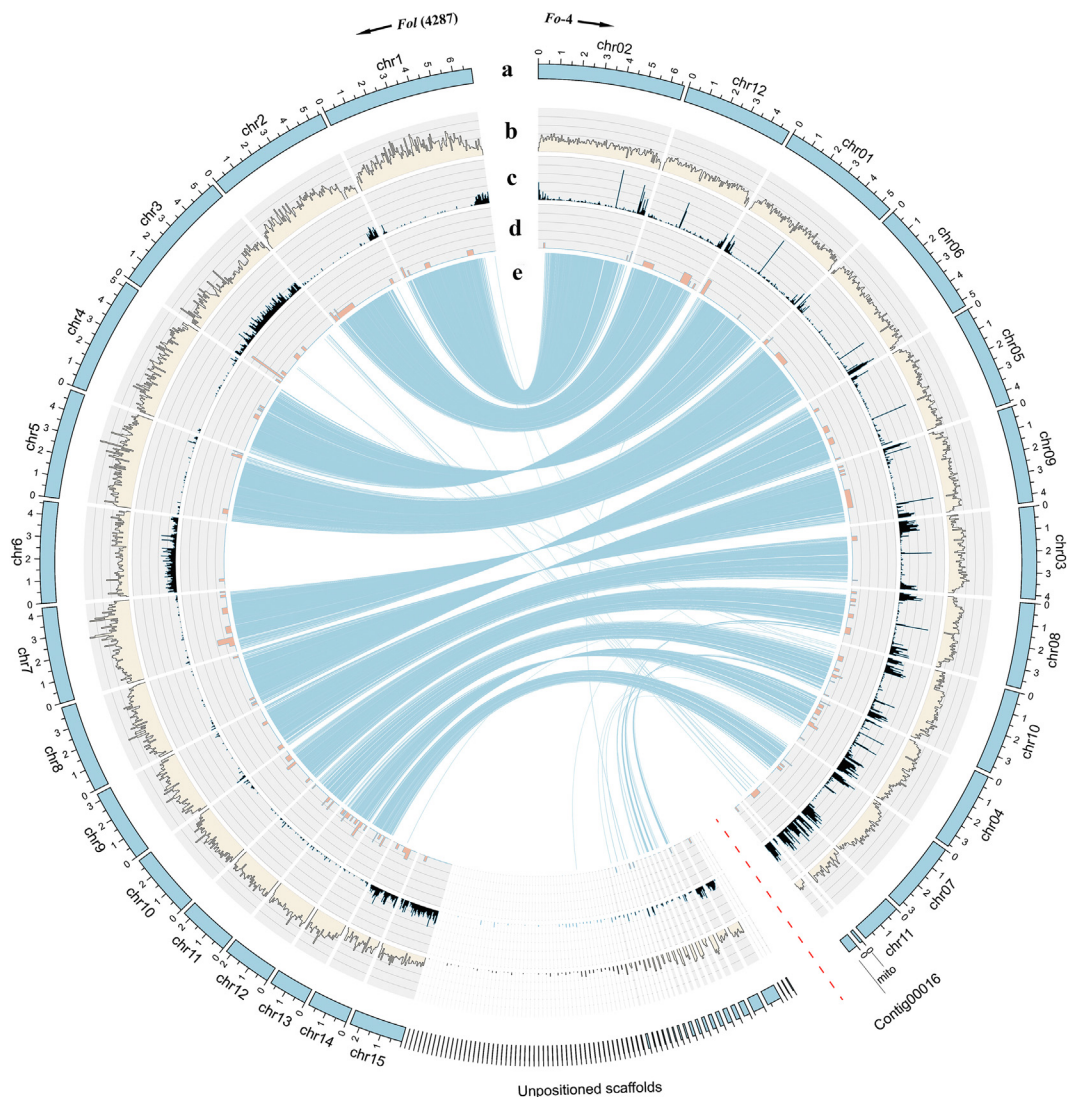


Fig. 1. Comparison of chromosomes between the *Fo-4* genome assembly and *Fol* (4287). **a** The *Fo-4* genome assembly, **b** Gene density, **c** Repeat sequence density, and **d** Candidate effector genes. Calculated in 50 kb windows. **e** Indicates nucleotide alignments with the *Fol* (4287) reference genome. Eleven conserved chromosomes were identified through synteny between *Fo-4* and *Fol* (4287), whereas chromosome 11 and contig00016 show reduced synteny.

supported our previous observations in which SA inhibited the hyphal growth and pathogenicity of *F. oxysporum*.

FoSAH1 significantly attenuates the SA sensitivity of *F. oxysporum*

SA is catalyzed by salicylate hydroxylase to generate biologically inactive catechol, resulting in a deficiency in SA accumulation and thus enabling the evasion of host plant defenses in phytopathogenic bacteria and fungi [37,38]. Because the IC_{50} of SA for *F. oxysporum* is much higher than that of chemical fungicide, we hypothesized that SA may be detoxified by salicylate hydroxylase in *F. oxysporum*. Sixteen putative salicylate hydroxylase (SAH) genes were found in the *F. oxysporum* genome using *Pseudomonas putida* NahG (salicylate hydroxylase) amino acid sequence as a reference, and *FoSAH1* (FOXG_09708) shared the highest similarity with PpNahG. Therefore, *FoSAH1* was selected for further study. The overall amino acid sequence identity was 36% between PpNahG and *FoSAH1* proteins. Sequence analysis results showed that *FoSAH1* was evolutionarily conserved. The FAD and NADH binding domain and substrate active site of *FoSAH1* were identified and highly conserved across various organisms (Fig. 4a). Analysis

of transcriptome data showed that the transcription level of *FoSAH1* was upregulated 10.15-fold in SA-treated hyphae. To further confirm the function of *FoSAH1*, *FoSAH1* deletion mutants ($\Delta Fosah1$) were created (Fig. S7). The $\Delta Fosah1$ mutant was more sensitive to SA than *Fo* and the complementary strain (Fig. 4b). The IC_{50} value of SA decreased to 1 mM in the $\Delta Fosah1$ mutant. Importantly, overexpression of *FoSAH1* strain displayed resistance to SA (Fig. 4c), and the transcription and protein levels of *FoSAH1* were significantly increased when hyphae were exposed to SA treatment (Fig. 4d and f), indicating that *FoSAH1* protein contributes to the detoxification of SA. The subcellular localization showed that *FoSAH1* was localized in the cytoplasm (Fig. 4e). Considering that *F. oxysporum* is an endophytic pathogen with 16 homologs of SAHs, they may play major roles in detoxifying SA to survive during long-term co-evolution between host and pathogens.

SA and RAP synergistically inhibit hyphal growth in *F. oxysporum*.

The growth retardation and deficiency of *F. oxysporum* resulting from SA treatment show similar features of target of rapamycin

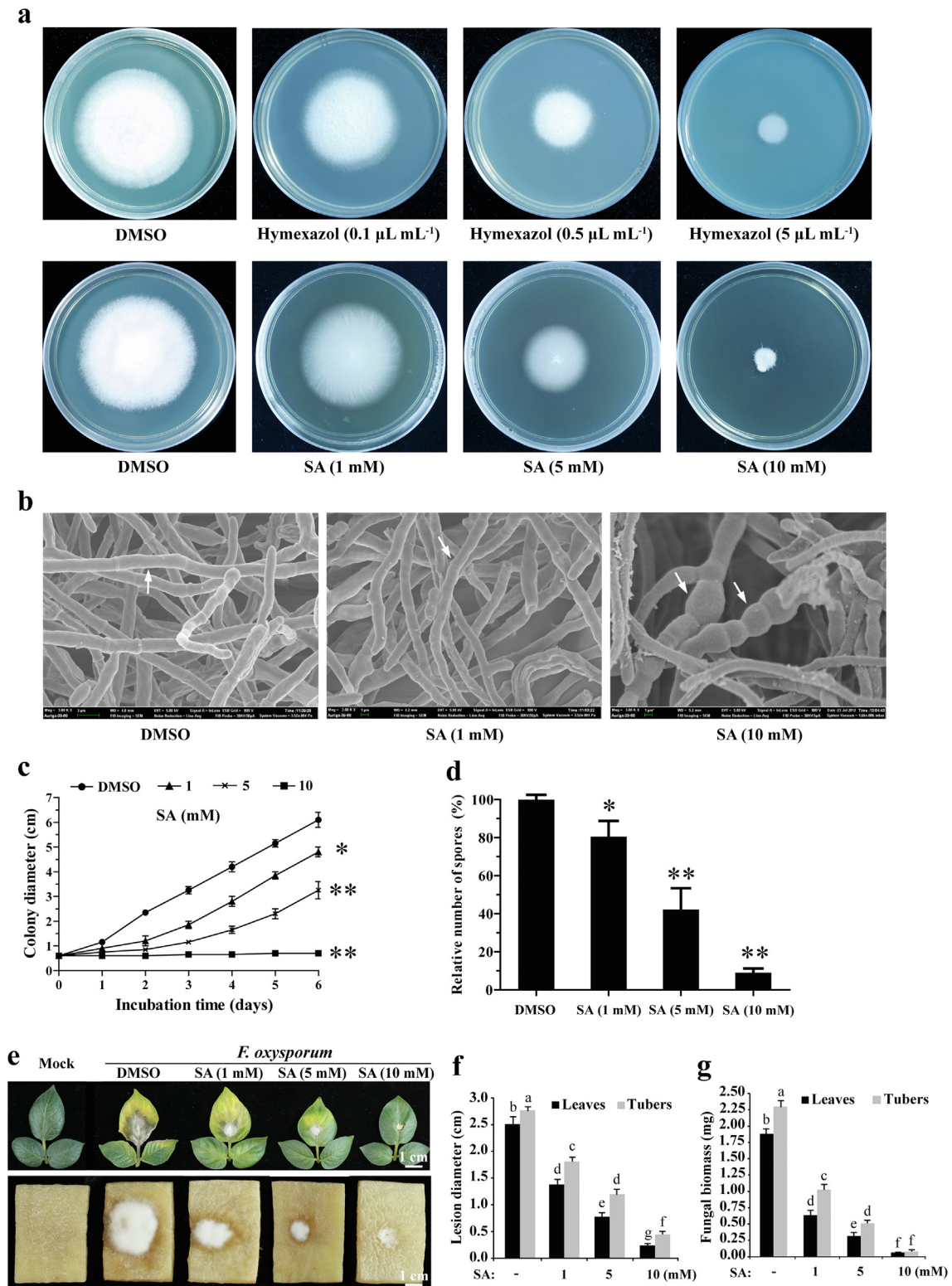


Fig. 2. SA inhibited the hyphal growth and pathogenicity of *F. oxysporum* in a dose-dependent manner. **a** SA mimics chemical fungicide to inhibit hyphae growth of *F. oxysporum*. Hyphae of *Fo-4* were incubated on PDA with different concentrations of hymexazol and SA for 6 days. **b** Growth defects of *Fo-4* generated by SA treatment. Hyphae of *Fo-4* were incubated on PDA with SA for 6 days and photographed by scanning electron microscopy. **c** Colony diameter of *Fo-4* treated with different concentrations of SA. **d** Spores production of *Fo-4*. Hyphae of *Fo-4* were incubated on PDA with SA for 6 days and then the spores were eluted with sterile water for counting. The data represents the mean \pm SD of $n = 3$ independent experiments. Asterisks denote student's t test significant difference compared with that of DMSO (* $P < 0.05$; ** $P < 0.01$). **e** SA inhibited the *Fusarium* wilt lesions caused by *F. oxysporum*. Spores of *Fo-4* mixing with different concentrations of SA were point-inoculated on the surface of potato leaves and tubers for 4 days. Potato leaves and tubers inoculated with water were used as a mock. Bar = 1 cm. **f** Lesion diameter of potato leaves and tubers as described in **e**. **g** Fungal biomass of *Fo-4* as described in **e**. The data represents the mean \pm SD of $n = 3$ independent experiments. Different letters represent significant differences between treatments (Tukey, $p < 0.05$).

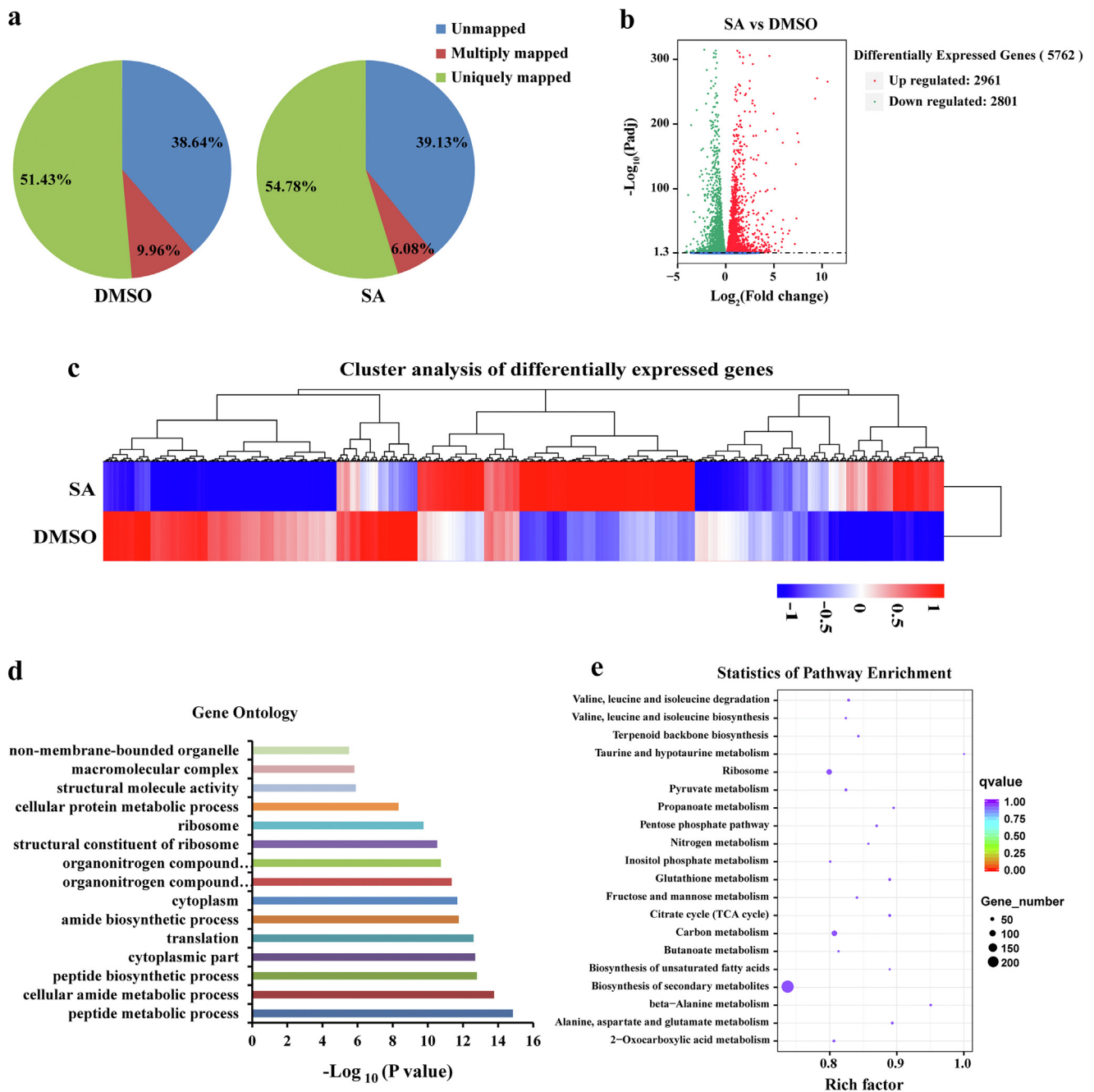


Fig. 3. RNA-seq analysis of *F. oxysporum* hyphae treated with DMSO and SA. **a** Proportions of clean reads of unmapped, multiply mapped, and uniquely mapped. **b** Number of downregulated and upregulated DEGs between SA and DMSO treatment. **c** Cluster analysis of DEGs between SA and DMSO treatment. **d** Significantly enriched gene ontology in SA treatment. Gene ontology was ranked by significance. **e** Significantly enriched pathways in SA treatment.

(TOR) pathway mutants [18]. It is well-known that TOR, evolutionarily conserved in all eukaryotes, acts as a master regulator of cell growth and proliferation [21,39,40]. Rapamycin (RAP) is a well-known TOR specific inhibitor, which negatively regulates TOR kinase activity. To assess the effect of RAP on TOR inhibition in *F. oxysporum*, we first assayed the sensitivity of the *Fo-4* strain to RAP (Fig. S8a). Growth inhibition of *F. oxysporum* was positively correlated with concentrations of RAP, and the IC_{50} value of RAP was 0.1 μ M. The pairwise combination of SA and RAP displayed more obvious growth inhibition than that treated with SA or RAP alone (Fig. S8b-d), and the IC_{50} value of single drug (SA: 1 mM; RAP: 10 nM) was drastically reduced when *F. oxysporum* was treated with SA and RAP combination, implying that potential synergistic effects can be generated by combining SA with RAP.

The computer-simulated Fa-CI curve was then assessed using the CompuSyn software. A synergistic effect ($CI < 1$) was observed when hyphae were treated with the combinations of SA + RAP (Fig. S8e), indicating that the combination of SA + RAP had a strong synergism. These results suggested that SA and RAP could inhibit hyphal growth by simultaneously targeting the TOR signaling pathway in *F. oxysporum*.

SA activates *FoSNF1* to inhibit *FoTORC1* signaling through *FoRAPTOR* phosphorylation

Previous reports have shown that phosphorylation of RAPTOR by AMPK is required for the inhibition of TORC1 in animals and humans [5,6,41]. To dissect the possible mechanism between SA

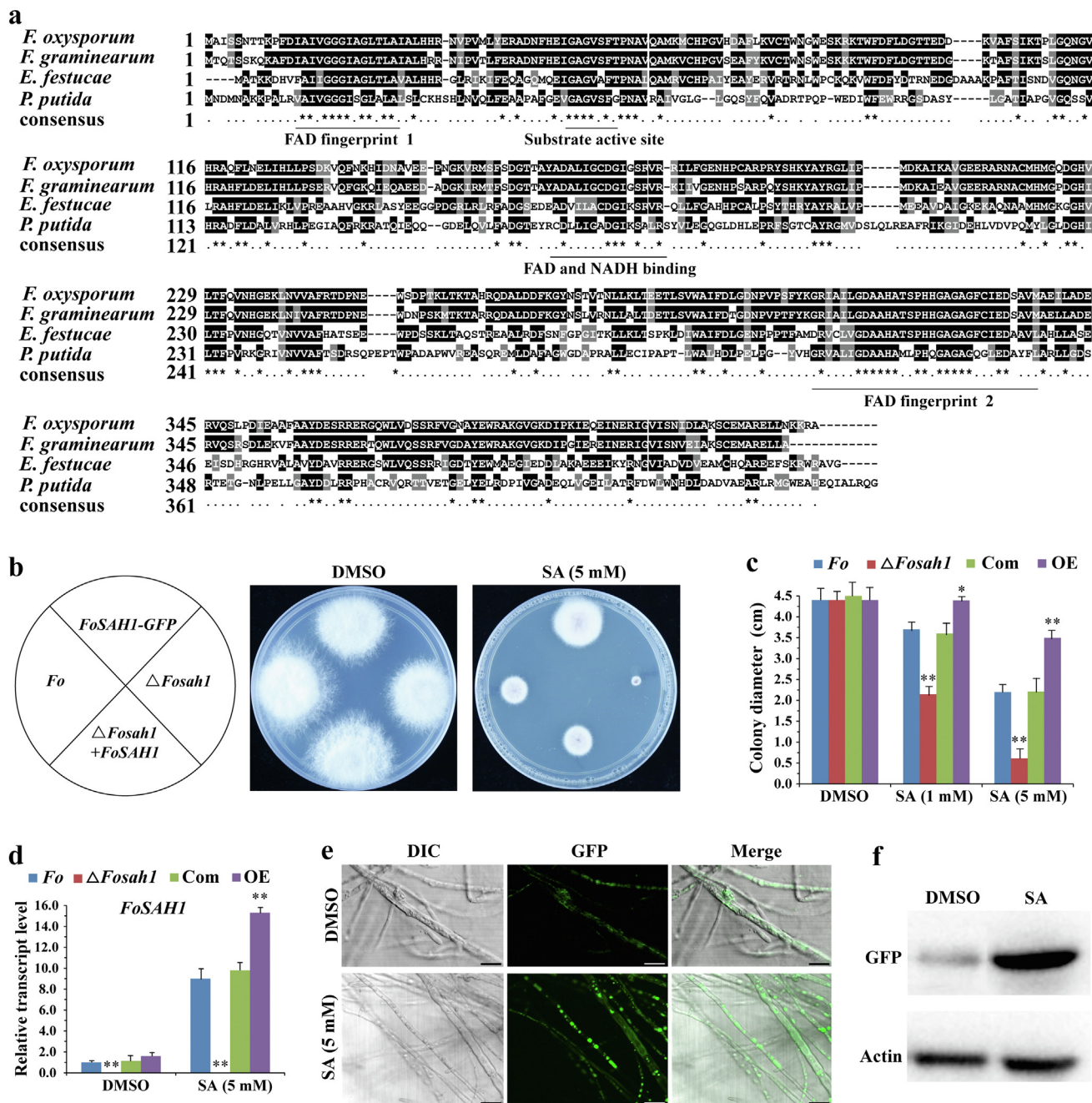


Fig. 4. Salicylate hydroxylase (FoSAHI) can effectively detoxify SA in *F. oxysporum*. **a** Comparison of amino acid sequences of FoSAHI protein with that of representative organisms including *F. graminearum*, *E. festucae*, and *P. putida*. Conserved domains were underlined. **b** Colony morphology of the Δ Fosah1 mutant and overexpression FoSAHI strains on PDA medium containing DMSO and SA for 4 days. **c** Colony diameter of *Fo*, Δ Fosah1, Com and OE strains treated with DMSO and SA for 4 days. OE, $P_{FoSAHI}::FoSAHI$ -GFP overexpression line; Com, Δ Fosah1 + FoSAHI complemented strain. **d** Transcript level of FoSAHI in *F. oxysporum* treated with SA. Hyphae of *Fo*, Δ Fosah1, Com and OE were incubated on PDA medium containing DMSO and SA grown for 4 days, respectively. *FoF1 α* was used as an internal control. The data represents the mean \pm SD of $n = 3$ independent experiments. Asterisks denote student's *t* test significant difference compared with that of *Fo* (* $P < 0.05$; ** $P < 0.01$). **e** Subcellular localization of FoSAHI in *F. oxysporum*. $P_{FoSAHI}::FoSAHI$ -GFP overexpression line was cultured on PDA medium containing DMSO (control) and SA grown for 4 days, respectively. GFP was photographed by laser confocal scanning microscope (OLYMPUS FLUOVIEW FV1200). Bars = 10 μ m. **f** Analysis of protein level of $P_{FoSAHI}::FoSAHI$ -GFP overexpression line by western blot as described in **e**. β -actin was used as an internal control.

and the TOR signaling pathway, we created FoSNF1 (also known as AMPK α) deletion mutants (Δ snf1), an upstream kinase of TORC1 [6]. Pharmacological assays showed that FoSNF1 deletion mutants were insensitive to SA compared with that of *Fo* (Fig. 5a), implying that FoSNF1 may be a key target of SA. Next, we assessed whether SA could activate FoSNF1. Sequences analysis found the conservation within the activation loops of FoSNF1, SpAMPK α^{Ssp2} and HsAMPK α [42] (Fig. 5b), the anti-Thr172 phospho-AMPK α anti-

body was thus used to recognize phosphorylated FoSNF1 at Thr223. SA increased the phosphorylation of FoSNF1 at Thr223, which reflected in FoSNF1 activity (Fig. 5c and d). Furthermore, FoSNF1 interacted with FoRAPTOR in yeast two-hybrid assay (Fig. 5e), and phosphorylation of FoRAPTOR was markedly increased in hyphae treated with SA (Fig. 5f). These results indicated that SA mediated the phosphorylation of FoRAPTOR by activating FoSNF1.

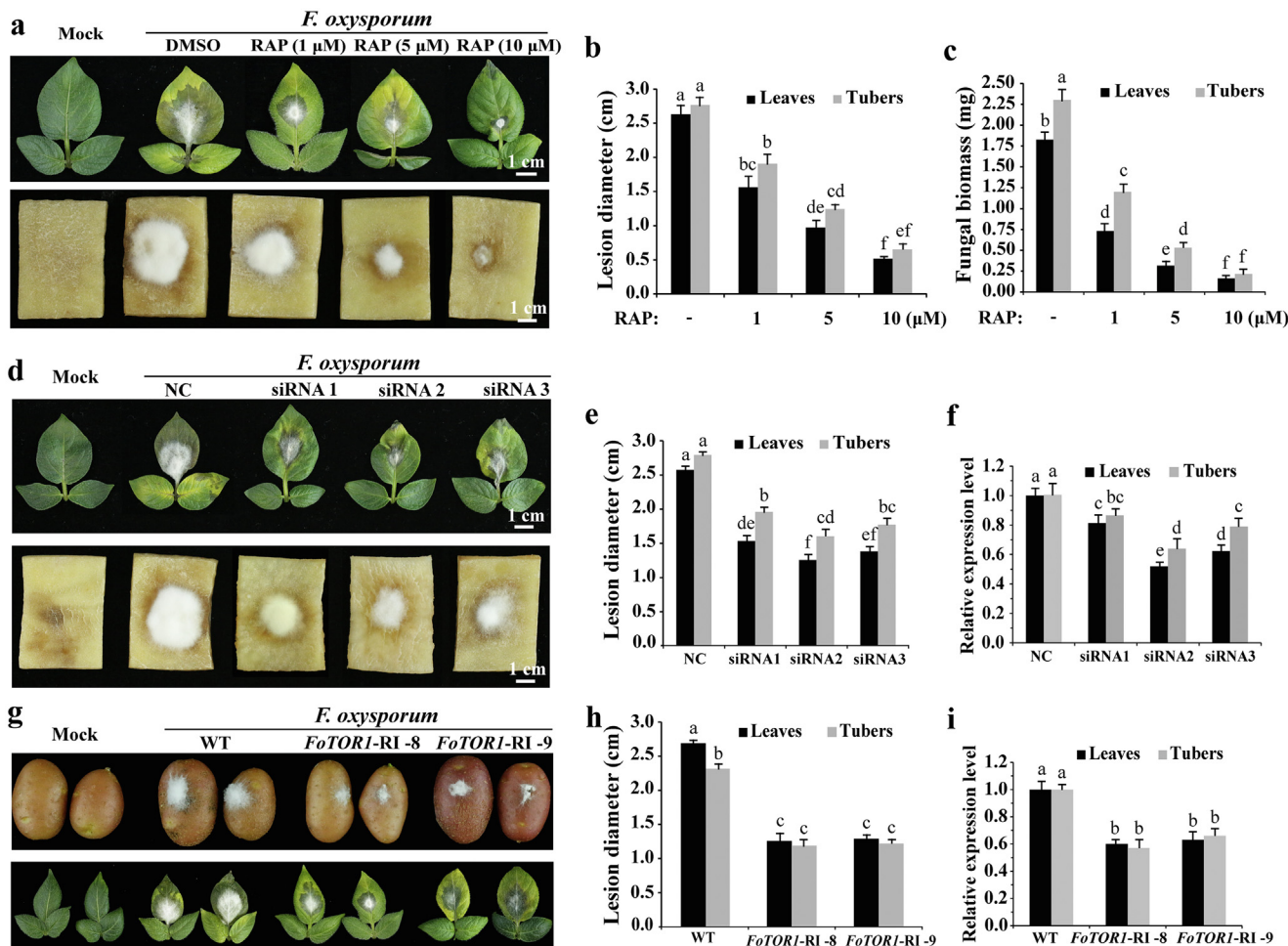


Fig. 6. Suppression of FoTOR1 protein activity can delay the onset of *Fusarium* wilt in potato leaves and tubers. **a** RAP inhibited the *Fusarium* wilt lesions caused by *F. oxysporum*. Spores of *Fo-4* mixing with different concentrations of RAP were point-inoculated on the surface of potato leaves and tubers for 4 days. Potato leaves and tubers inoculated with water were used as mock. Bar = 1 cm. **b** Lesion diameter of potato leaves and tubers as described in **a**. **c** Fungal biomass of *Fo-4* as described in **a**. **d** siRNAs of *FoTOR1* significantly inhibited the mycelial growth of *F. oxysporum*. Spores of *Fo-4* mixing with *FoTOR1* siRNAs were point-inoculated on the surface of potato leaves and tubers for 4 days. Spores of *Fo-4* mixing with random siRNA were used as a negative control (NC). **e** Lesion diameter of potato leaves and tubers as described in **d**. **f** Relative expression level of the *FoTOR1* gene as described in **d**. **g** Transgenic *FoTOR1*-RI potato plants were resistant to *Fusarium* wilt. Spores of *Fo-4* were point-inoculated on the surface of transgenic *FoTOR1*-RI potato leaves and tubers for 4 days. Potato (WT) leaves and tubers were point-inoculated with conidial suspension of *Fo-4* as a positive control. **h** Lesion diameter of transgenic *FoTOR1*-RI potato leaves and tubers as described in **g**. **i** Relative expression level of the *FoTOR1* gene as described in **g**. *FoEF1α* was used as an internal control. The data represents the mean ± SD of n = 3 independent experiments. Different letters represent significant differences between treatments (Tukey, p < 0.05).

RAPTOR is known to recruit substrates to TOR kinase and is required for the regulation of TORC1 activity [43]. RAPTOR phosphorylation inhibits TORC1 activity [6,44]. In order to verify whether phosphorylated FoRAPTOR inhibits the activity of FoTORC1, we detected the phosphorylation of RPS6 (ribosomal protein S6) at Ser 235/236, which is the output of TOR signaling and is essential for protein synthesis and cell cycle progression [45]. As expected, the phosphorylation level of FoRPS6 at Ser 235/236 was decreased in hyphae with SA treatment (Fig. 5g), which indicated a decrease in TORC1 activity. These results suggested that SA exerts an inhibitory effect on TORC1 signaling by activating FoSNF1 in *F. oxysporum*.

Suppression of FoTOR1 protein activity in vivo and in vitro can block the occurrence of Fusarium wilt in potatoes

We next tested the pathogenicity of *F. oxysporum* under FoTOR1 inhibition in potato. Spores were mixed with different concentrations of RAP and then point-inoculated on the surface of potato leaves and tubers. Consistently, RAP inhibited *Fusarium* wilt lesions

caused by *F. oxysporum* in a dose-dependent manner as described in SA, which reflected less biomass of the fungus, smaller necrosis symptoms, and slower yellowing and wilting (Fig. 6a-c). To further confirm that *FoTOR1* (*FOXG_02818*) interference can inhibit the mycelial growth and pathogenicity of *F. oxysporum*, we synthesized siRNAs that specifically targeted the *FoTOR1* gene *in vitro* (Table S6). All siRNAs of *FoTOR1* significantly inhibited the mycelial growth of *F. oxysporum* (Fig. 6d and e). Furthermore, the *FoTOR1* mRNA level of *F. oxysporum* decreased in response to *FoTOR1* siRNAs treatment (Fig. 6f and Fig. S9b). These results suggested that FoTOR1 is a key target for the control of *Fusarium* wilt in potatoes.

Next, transgenic *FoTOR1* and *FoSAH1* RNA interference (RNAi) potato plants were generated using agrobacterium-mediated transformation approach. Independent transgenic RNAi potato plants that carry *FoTOR1*-RI, *FoSAH1*-RI, and *FoTOR1* + *FoSAH1*-RI fragments were obtained (Table S7). Phenotypic analyses showed that all transgenic potato plants were indistinguishable from wild-type plants. Most of the transgenic potato plants were resistant to *Fusarium* wilt (Table S7). The transgenic *FoTOR1*-RI potato plants significantly inhibited mycelial growth and reduced the

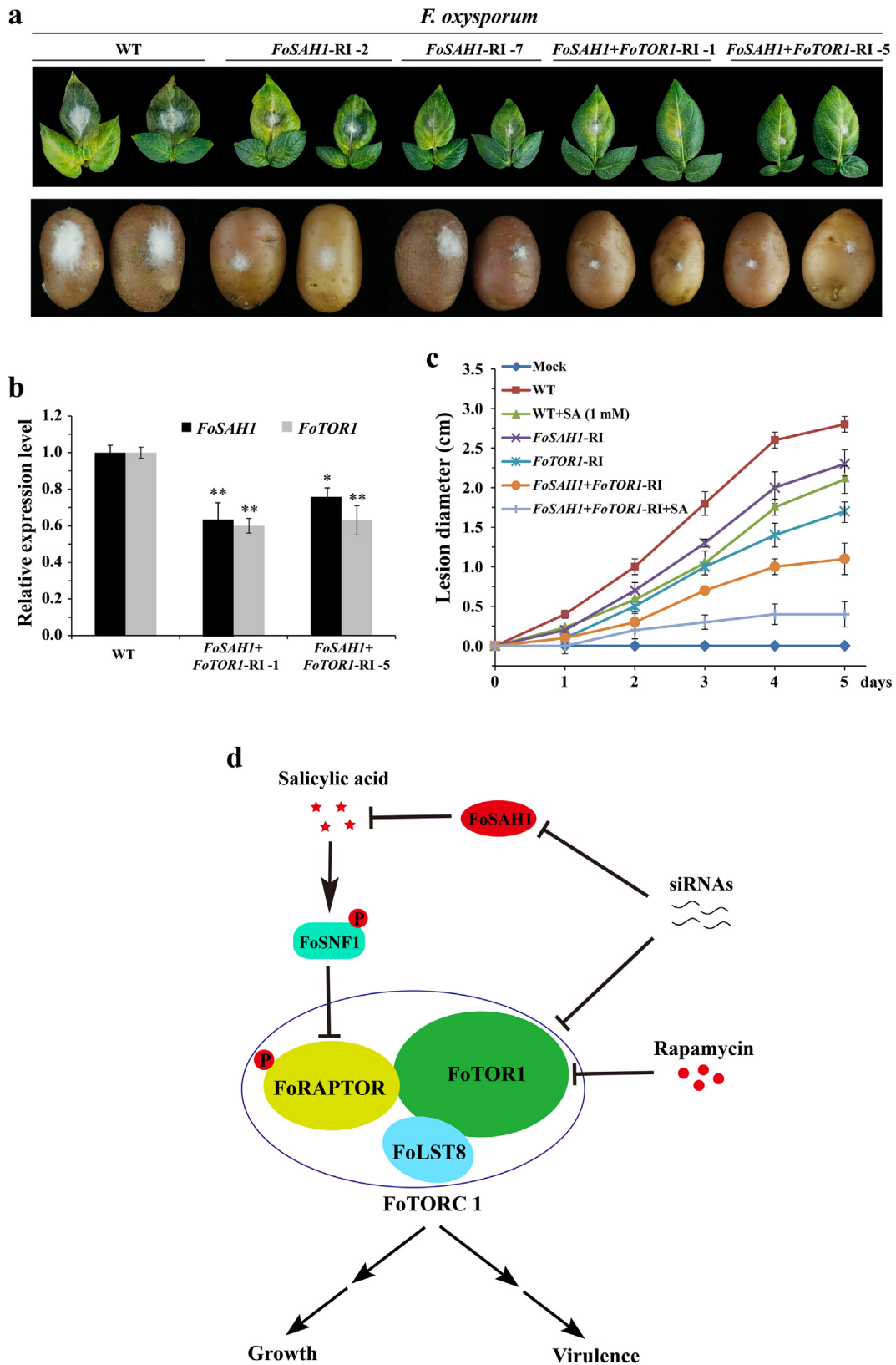


Fig. 7. Transgenic potato plants with interference of *FoSAH1* and *FoTOR1* genes were resistant to *Fusarium* wilt and dry rot. **a** Transgenic *FoSAH1*-RI and *FoSAH1* + *FoTOR1*-RI potato plants were resistant to *Fusarium* wilt and dry rot. Spores of *Fo-4* were point-inoculated on the surface of transgenic *FoSAH1*-RI and *FoSAH1* + *FoTOR1*-RI potato leaves and tubers for 4 days. Potato (WT) leaves and tubers were point-inoculated with conidial suspension of *Fo-4* as a positive control. **b** Relative expression levels of *FoSAH1* and *FoTOR1* genes as described in **a**. *FoEF1α* was used as an internal control. The data represents the mean ± SD of n = 3 independent experiments. Asterisks denote student's *t* test significant difference compared with that of WT (**P* < 0.05; ***P* < 0.01). **c** Lesion diameter of transgenic *FoSAH1*-RI, *FoTOR1*-RI, and *FoSAH1* + *FoTOR1*-RI potato leaves. Spores of *Fo-4* mixing with or without SA (1 mM) were point-inoculated on the surface of transgenic potato leaves and tubers for 4 days. Potato (WT) leaves inoculated with water were used as a negative control (Mock). The data represents the mean ± SD of n = 3 independent experiments. **d** A simplified model shows that SA regulates growth and pathogenicity through *FoTORC1* in *F. oxysporum*. In this model, salicylic acid, rapamycin, and siRNAs suppress the activity of *FoTORC1*. *FoTORC1* positively controls the expression of growth and virulence genes. Arrows and T-bars represent enhancement and inhibition, respectively.

pathogenicity of *F. oxysporum*, which conferred resistance against *Fusarium* wilt on potato leaves and tubers (Fig. 6g and h). Furthermore, the *TOR1* mRNA level of *F. oxysporum* was significantly decreased after incubation with transgenic *FoTOR1*-RI potato plants (Fig. 6i and Fig. S9c). Consistent with *FoTOR1* interference, *FoSAH1*-RI plants were resistant to *F. oxysporum*, and *FoTOR1* + *FoSAH1*-RI plants displayed a smaller lesion size than *FoTOR1*-RI or *FoSAH1*-RI plants alone (Fig. 7a). The expression levels of *FoSAH1* and *FoTOR1* genes were significantly decreased in the *FoTOR1* + *FoSAH1*-RI plants (Fig. 7b and Fig. S9d). Additionally, transgenic *FoTOR1*/*FoSAH1*-RI RNAi potato plants plus exogenous SA significantly reduced the pathogenicity of *F. oxysporum* compared with that of *FoTOR1*/*FoSAH1*-RI RNAi potato plants or exogenous SA treatment alone (Fig. 7c and Fig. S10). These results suggested that suppression of *FoTOR1* protein activity or reduction of *FoTOR1* and *FoSAH1* mRNA levels by RNAi could inhibit mycelial growth and decrease the pathogenicity of *F. oxysporum* in potato plants.

Discussion

Fusarium wilt is a major phytopathogenic disease affecting more than 100 economically important crops, such as potato, tomato, banana, cotton and melon, and many horticultural crops [15,16,46]. *Fusarium oxysporum* is the major shared pathogen in various *Fusarium* wilt diseases and is ranked fifth in a survey of the Top 10 fungal plant pathogens [47]. *Forma specialis* of *F. oxysporum* typically has a narrow host range among species, but a few *forma specialis* show an extended host range among genera [48]. Expanding the host range by horizontal chromosome transfer between different *forma specialis* of *F. oxysporum* makes the pathogen more deadly [16,48]. In this study, *Fo-4* displayed much broader host ranges among families from *Solanaceae*, *Vitaceae*, *Musaceae*, *Cucurbitaceae* to *Dioscoreaceae* than other *forma specialis* of *F. oxysporum*. As far as we know, *Fo-4* is the most infectious pathogenic *F. oxysporum*. To explore the underlying reasons why *Fo-4* had the broader host ranges, we sequenced the *Fo-4* genome. The results showed that *Fo-4* had 12 chromosomes, of which chromosome 11 included the most repetitive sequences and many pathogenic secreted proteins. However, whether the chromosome 11 is a pathogenicity chromosome that infects more hosts requires further study.

Due to the lack of varieties resistant to *Fusarium* wilt and efficient biofungicides, the control of this disease largely depends on high dosage and high frequency of chemical fungicide applications. However, these chemical fungicides face increasing challenges, including limited efficacy, environmental contamination, and drug resistance development. Thus, effective, safe, and eco-friendly biological fungicides are urgently needed to replace the chemical fungicides in the agricultural industry and sustainable development. Development of these new biofungicides would promote environmental protection, sustainability, and improve human health. However, so far, few useful biological fungicides have been developed against *Fusarium* wilt [17]. In this study, we discovered that SA, which was induced by stresses and natively produced by plants [49,50], can directly inhibit *F. oxysporum* cells and significantly prevent the occurrence of potato *Fusarium* wilt. Importantly, we found that SA showed potent inhibitory activity against *F. oxysporum* by targeting the *FoTOR* signaling pathway. *TOR* is a key lethal gene with a large molecular weight (280 KD) and multiple functional domains [20,51]. *TOR* signaling operates as a master input/output node that mediates various upstream signal cascades for modulating cell growth, development, proliferation, and death in all examined eukaryotic organisms [40,52,53]. We further found that *FoSNF1* can mediate SA to inhibit the activity of *FoTORC1* by phosphorylating *FoRAPTOR*. Thus, the *FoSNF1*-*FoTORC1* signaling

cascade is an ideal target for high-throughput screening of potential biofungicides such as SA against *Fusarium* wilt. Besides, the RNA-seq data showed that SA affects multiple metabolic pathways, especially in the MAPK cascade and CWDEs, indicating that SA targets multiple signaling pathways in *F. oxysporum*. These observations provide new insights into that SA is not only a defensive weapon, but also an offensive weapon against fungal pathogens.

Fusarium oxysporum is a hemibiotrophic and endophytic pathogen feeding on plant cells [54]. In our results, SA can be used as an offensive weapon to damage *F. oxysporum* cells. To successfully colonize and survive in plant cells, *F. oxysporum* must spatiotemporally deploy and evolve strong SAHs to degrade SA in plants. More than 16 SAHs were found in *F. oxysporum*, which was higher than that of other phytopathogenic fungi (Table S8). Diverse and rapid evolution of *FoSAHs* during long-term co-evolution between host and the pathogen may be the reason why *F. oxysporum* can successfully infect over 100 plants. Transgenic *Arabidopsis* with the bacterium *Pseudomonas putida* salicylate hydroxylase gene can decompose SA, leading to lower resistance to pathogens [37], indicating that salicylate hydroxylase has functions in plants. It is possible that the engineered plants with enough siRNAs of *FoSAHs* may significantly block the invasion and colonization of *F. oxysporum* in the vascular part of plants.

We therefore propose a model to highlight the role of exogenous SA in regulating hyphal growth and pathogenicity via the *FoSNF1*-*FoTORC1* signaling pathway in *F. oxysporum* (Fig. 7d). Phytohormone SA, produced by plants, inhibits the activity of *FoTORC1* by phosphorylating *FoSNF1*, resulting in the arrest of growth and reduction of pathogenicity of *F. oxysporum*, whereas the endogenous salicylate hydroxylases (*FoSAHs*) attenuate the toxicity of SA by detoxifying SA. The mycelial growth, cell viability, and virulence of *F. oxysporum* were synergistically inhibited when SA was combined with *TOR* inhibitors such as rapamycin and siRNAs of *FoTOR1*. Thus, a efficient *FoTOR* signaling inhibition system was established for controlling *F. oxysporum*. Especially, SA and siRNAs of *FoTOR1* and *FoSAH1* genes can be engineered and produced by plants [55,56]. Considering that *TOR* is a lethal gene in various eukaryotic pathogens from plants to animals and humans, the synergistic effects generated by SA and *TOR* inhibitors may contribute to therapies for various fungal diseases from plants to animals and humans. Hopefully, *F. oxysporum* pathogen can be successfully controlled by applying SA and siRNAs of *FoTOR1* and *FoSAH1* genes in crops in the future. Crop cultivars sustainably resistant to *Fusarium* wilt may be generated by inducing and enhancing SA and siRNAs of *FoTOR1* and *FoSAH1* genes in crops.

Compliance with Ethics Requirement

This article does not contain any studies with human or animal subjects.

Declaration of Competing Interest

The authors declare that they have no known competing financial interests or personal relationships that could have appeared to influence the work reported in this paper.

Acknowledgements

MR and LL designed the experiments. LL, TZ, YS and LF performed the experiments. LL, TZ, RD and YS analyzed the data. MR, LL, TZ, YS, PK, RR and MS wrote the manuscript. This work was supported by grants from the National Natural Science Foundation of China (No. 32002105 and 31972469) and Agricultural Science and Technology Innovation Program of Chinese Academy of Agricultural Sciences (34-IUA-02).

Appendix A. Supplementary material

Supplementary data to this article can be found online at <https://doi.org/10.1016/j.jare.2021.10.014>.

References

- Chambers JE, Greim H, Kendall RJ, Segner H, Sharpe RM, Van Der Kraak G. Human and ecological risk assessment of a crop protection chemical: a case study with the azole fungicide epoxiconazole. *Crit Rev Toxicol* 2014;44(2):176–210.
- Stamatis N, Hela D, Konstantinou I. Occurrence and removal of fungicides in municipal sewage treatment plant. *J Hazard Mater* 2010;175(1-3):829–35.
- Norn S, Permin H, Kruse PR, Kruse E. From willow bark to acetylsalicylic acid. *Dan Medicinhist Arbog* 2009;37:79–98.
- Klessig DF, Tian M, Choi HW. Multiple Targets of Salicylic Acid and Its Derivatives in Plants and Animals. *Front Immunol* 2016;7:206.
- Hawley SA, Fullerton MD, Ross FA, Schertzer JD, Chevtzoff C, Walker KJ, et al. The ancient drug salicylate directly activates AMP-activated protein kinase. *Science* 2012;336(6083):918–22.
- Gwinn DM, Shackelford DB, Egan DF, Mihaylova MM, Mery A, Vasquez DS, et al. AMPK phosphorylation of raptor mediates a metabolic checkpoint. *Mol Cell* 2008;30(2):214–26.
- Ding Y, Sun T, Ao K, Peng Y, Zhang Y, Li X, et al. Opposite Roles of Salicylic Acid Receptors NPR1 and NPR3/NPR4 in Transcriptional Regulation of Plant Immunity. *Cell* 2018;173(6):1454–1467.e15.
- Radojicic A, Li X, Zhang Y. Salicylic Acid: A Double-Edged Sword for Programmed Cell Death in Plants. *Front Plant Sci* 2018;9:1133.
- Amborabé B-E, Fleurat-Lessard P, Chollet J-F, Roblin G. Antifungal effects of salicylic acid and other benzoic acid derivatives towards *Eutypa lata*: structure–activity relationship. *Plant Physiol Bioch* 2002;40(12):1051–60.
- da Rocha Neto AC, Maraschin M, Di Piero RM. Antifungal activity of salicylic acid against *Penicillium expansum* and its possible mechanisms of action. *Int J Food Microbiol* 2015;215:64–70.
- Daw BD, Zhang LH, Wang ZZ. Salicylic acid enhances antifungal resistance to *Magnaporthe oryzae* in rice plants. *Australas Plant Path* 2008;37(6):637–44.
- Wu HS, Raza W, Fan JQ, Sun YG, Bao W, Liu DY, et al. Antibiotic effect of exogenously applied salicylic acid on *in vitro* soilborne pathogen, *Fusarium oxysporum* f.sp.niveum. *Chemosphere* 2008;74(1):45–50.
- Ma L-J, van der Does HC, Borkovich KA, Coleman JJ, Daboussi M-J, Di Pietro A, et al. Comparative genomics reveals mobile pathogenicity chromosomes in *Fusarium*. *Nature* 2010;464(7287):367–73.
- Gordon TR. *Fusarium oxysporum* and the *Fusarium* Wilt Syndrome. *Annu Rev Phytopathol* 2017;55(1):23–39.
- García Bayona L, Grajales A, Cárdenas ME, Sierra R, Lozano G, Garavito MF, et al. Isolation and characterization of two strains of *Fusarium oxysporum* causing potato dry rot in *Solanum tuberosum* in Colombia. *Rev Iberoam Micol* 2011;28(4):166–72.
- Husaini AM, Sakina A, Cambay SR. Host-pathogen interaction in *Fusarium oxysporum* infections: where do we stand? *Mol Plant Microbe Interact* 2018;31(9):889–98.
- Raza W, Ling N, Zhang R, Huang Q, Xu Y, Shen Q. Success evaluation of the biological control of *Fusarium* wilts of cucumber, banana, and tomato since 2000 and future research strategies. *Crit Rev Biotechnol* 2017;37(2):202–12.
- De Virgilio C, Loewith R. Cell growth control: little eukaryotes make big contributions. *Oncogene* 2006;25(48):6392–415.
- Yuan H-X, Xiong Y, Guan K-L. Nutrient Sensing, Metabolism, and Cell Growth Control. *Mol Cell* 2013;49(3):379–87.
- González A, Hall MN. Nutrient sensing and TOR signaling in yeast and mammals. *EMBO J* 2017;36(4):397–408.
- Loewith R, Jacinto E, Wullschleger S, Lorberg A, Crespo JL, Bonenfant D, et al. Two TOR complexes, only one of which is rapamycin sensitive, have distinct roles in cell growth control. *Mol Cell* 2002;10(3):457–68.
- Hara K, Maruki Y, Long X, Yoshino K-I, Oshiro N, Hidayat S, et al. Raptor, a binding partner of target of rapamycin (TOR), mediates TOR action. *Cell* 2002;110(2):177–89.
- Heitman J, Movva NR, Hall MN. Targets for cell cycle arrest by the immunosuppressant rapamycin in yeast. *Science* 1991;253(5022):905–9.
- Ruan J, Li H. Fast and accurate long-read assembly with wtdbg2. *Nat Methods* 2020;17(2):155–8.
- Simão FA, Waterhouse RM, Ioannidis P, Kriventseva EV, Zdobnov EM. BUSCO: assessing genome assembly and annotation completeness with single-copy orthologs. *Bioinformatics* 2015;31(19):3210–2.
- Burton JN, Adey A, Patwardhan RP, Qiu R, Kitzman JO, Shendure J. Chromosome-scale scaffolding of *de novo* genome assemblies based on chromatin interactions. *Nat Biotechnol* 2013;31(12):1119–25.
- Brankovics B, Zhang H, van Diepening AD, Ta VDL, Waalwijk C, de Hoog GS. GRAB: Selective Assembly of Genomic Regions, a New Niche for Genomic Research. *PLoS Comput Biol* 2016;12(6):e1004753.
- Luo X, Mao H, Wei Y, Cai J, Xie C, Sui A, et al. The fungal-specific transcription factor VdPfl influences conidia production, melanized microsclerotia formation, and pathogenicity in *Verticillium dahliae*. *Mol Plant Pathol* 2016;17(9):1364–81.
- Mao X, Cai T, Olyarchuk JG, Wei L. Automated genome annotation and pathway identification using the KEGG Orthology (KO) as a controlled vocabulary. *Bioinformatics* 2005;21(19):3787–93.
- Chou T-C. Theoretical basis, experimental design, and computerized simulation of synergism and antagonism in drug combination studies. *Pharmacol Rev* 2006;58(3):621–81.
- Thatcher LF, Manners JM, Kazan K. *Fusarium oxysporum* hijacks COI1-mediated jasmonate signaling to promote disease development in *Arabidopsis*. *Plant J* 2009;58(6):927–39.
- Hamel L-P, Nicole M-C, Duplessis S, Ellis BE. Mitogen-activated protein kinase signaling in plant-interacting fungi: distinct messages from conserved messengers. *Plant Cell* 2012;24(4):1327–51.
- Di Pietro A, García-MacEira FI, Méglez E, Roncero MI. A MAP kinase of the vascular wilt fungus *Fusarium oxysporum* is essential for root penetration and pathogenesis. *Mol Microbiol* 2001;39(5):1140–52.
- Segorbe D, Di Pietro A, Pérez-Nadales E, Turrà D. Three *Fusarium oxysporum* mitogen-activated protein kinases (MAPKs) have distinct and complementary roles in stress adaptation and cross-kingdom pathogenicity. *Mol Plant Pathol* 2017;18(7):912–24.
- Quoc NB, Chau NNB. The Role of Cell Wall Degrading Enzymes in Pathogenesis of *Magnaporthe oryzae*. *Curr Protein Pept Sci* 2017;18(10):1019–34.
- Ospina-Giraldo MD, Mullins E, Kang S. Loss of function of the *Fusarium oxysporum* SNF1 gene reduces virulence on cabbage and *Arabidopsis*. *Curr Genet* 2003;44(1):49–57.
- Delaney TP, Uknes S, Vernooij B, Friedrich L, Weymann K, Negrotto D, et al. A central role of salicylic acid in plant disease resistance. *Science* 1994;266(5188):1247–50.
- Fang Yi, Bullock H, Lee SA, Sekar N, Eiteman MA, Whitman WB, et al. Detection of methyl salicylate using bi-enzyme electrochemical sensor consisting salicylate hydroxylase and tyrosinase. *Biosens Bioelectron* 2016;85:603–10.
- Dobrenel T, Caldana C, Hanson J, Robaglia C, Vincenz M, Veit B, et al. TOR Signaling and Nutrient Sensing. *Annu Rev Plant Biol* 2016;67(1):261–85.
- Saxton RA, Sabatini DM. mTOR Signaling in Growth, Metabolism, and Disease. *Cell* 2017;168(6):960–76.
- Din FVN, Valanciute A, Houde VP, Zibrova D, Green KA, Sakamoto K, et al. Aspirin inhibits mTOR signaling, activates AMP-activated protein kinase, and induces autophagy in colorectal cancer cells. *Gastroenterology* 2012;142(7):1504–1515.e3.
- Davie, Elizabeth, Forte, Gabriella, Nbsp, M.A, et al. Nitrogen Regulates AMPK to Control TORC1 Signaling. *Curr Biol* 2015;25(4):445–54.
- Kim Do-Hyung, Sarbassov Dos D, Ali Siraj M, King Jessie E, Latek Robert R, Erdjument-Bromage Hediye, et al. mTOR interacts with Raptor to form a nutrient-sensitive complex that signals to the cell growth machinery. *Cell* 2002;110(2):163–75.
- Dunlop Elaine A, Hunt David K, Acosta-Jaquez Hugo A, Fingar Diane C, Tee Andrew R. ULK1 inhibits mTORC1 signaling, promotes multisite Raptor phosphorylation and hinders substrate binding. *Autophagy* 2011;7(7):737–47.
- Chauvin C, Koka V, Nouschi A, Mieulet V, Hoareau-Aveilla C, Drezean A, et al. Ribosomal protein S6 kinase activity controls the ribosome biogenesis transcriptional program. *Oncogene* 2014;33(4):474–83.
- Ploetz Randy C. *Fusarium* Wilt of Banana. *Phytopathology* 2015;105(12):1512–21.
- Dean R, Van Kan JA, Pretorius ZA, Hammondkosack KE, Di PA, Spanu PD, et al. The Top 10 fungal pathogens in molecular plant pathology. *Mol Plant Pathol* 2012;13(4):804.
- van Dam Peter, Fokkens Like, Ayukawa Yu, van der Gragt Michelle, ter Horst Anneliek, Brankovics Balázs, et al. A mobile pathogenicity chromosome in *Fusarium oxysporum* for infection of multiple cucurbit species. *Sci Rep* 2017;7(1). doi: <https://doi.org/10.1038/s41598-017-07995-y>.
- Vlot A Corina, Dempsey D'Maris Amick, Klessig Daniel F. Salicylic Acid, a multifaceted hormone to combat disease. *Annu Rev Phytopathol* 2009;47(1):177–206.
- Liu X, Rockett KS, Korner CJ, Pajeroska-Mukhtar KM. Salicylic acid signalling: new insights and prospects at a quarter-century milestone. *Essays Biochem* 2015;58:101–13.
- Yang Haijuan, Rudge Derek G, Koos Joseph D, Vaidialingam Bhamini, Yang Hyo J, Pavletich Nikola P. mTOR kinase structure, mechanism and regulation. *Nature* 2013;497(7448):217–23.
- Yu F, Gu Q, Yun Y, Yin Y, Xu JR, Shim WB, et al. The TOR signaling pathway regulates vegetative development and virulence in *Fusarium graminearum*. *New Phytol* 2014;203(1):219–32.
- Li Linxuan, Zhu Tingting, Song Yun, Luo Xiemei, Datla Raju, Ren Maozhi. Target of rapamycin controls hyphal growth and pathogenicity through FoTIP4 in *Fusarium oxysporum*. *Mol Plant Pathol* 2021;22(10):1239–55.
- Lyons R, Stiller J, Powell J, Rusu A, Manners JM, Kazan K. *Fusarium oxysporum* triggers tissue-specific transcriptional reprogramming in *Arabidopsis thaliana*. *PLoS One* 2015;10(4):e0121902.
- Wang M, Weiberg A, Lin FM, Thomma BPHJ, Huang HD, Jin H. Bidirectional cross-kingdom RNAi and fungal uptake of external RNAs confer plant protection. *Nat Plants* 2016;2(10):16151.
- Cai Qiang, Qiao Lulu, Wang Ming, He Baoye, Lin Feng-Mao, Palmquist Jared, et al. Plants send small RNAs in extracellular vesicles to fungal pathogen to silence virulence genes. *Science* 2018;360(6393):1126–9.